

Chapter 2: Resonances

Sagredo—Even as a boy, I observed that one man alone by giving these impulses at the right instant was able to ring a bell so large that when four, or even six, men seized the rope and tried to stop it they were lifted from the ground, all of them together being unable to counterbalance the momentum which a single man, by properly-timed pulls, had given it.

Salviati—Your illustration [can also] explain the wonderful phenomenon of the strings of the cittern or the spinet, namely, that a vibrating string will set another string in motion and cause it to sound... these vibrations cause the immediately surrounding air to vibrate and quiver; then these ripples in the air expand far into space and strike not only all the strings of the same instrument but even those of neighboring instruments.

Galileo Galilei, *Two New Sciences*

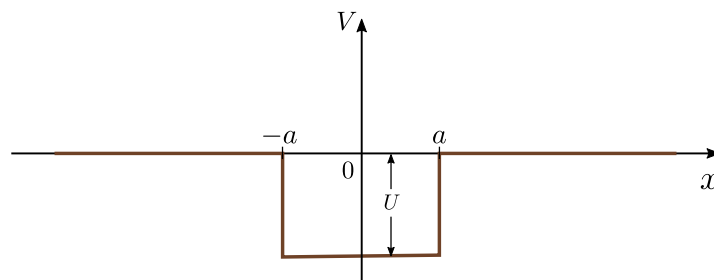
2.1. BOUND STATES AND FREE STATES

A curious feature of wavefunctions in infinite space is that they come in two distinct varieties: (i) **bound states** that are localized to one region, like the ground state of a harmonic oscillator, and (ii) **free states** that extend over all space, like a plane wave.

Both kinds of states can co-exist in a single system. This is demonstrated by a simple model called the **1D finite square well**, whose Hamiltonian is

$$\hat{H} = \frac{\hat{p}^2}{2m} - U \Theta(a - |\hat{x}|), \quad (2.1)$$

where \hat{x} and \hat{p} are 1D position and momentum operators, m is the particle mass, U and a are positive real parameters, and Θ denotes the step function (i.e., 1 if the input is positive, and 0 otherwise). As shown below, the potential well has depth U and width $2a$.



We can solve the time-independent Schrödinger wave equation for this Hamiltonian using a simple technique called the **transfer matrix method**. Some key aspects of the calculation are described below; the rest of the details are given in **Appendix B**.

Outside the potential well, the Schrödinger wave equation reduces to

$$-\frac{\hbar^2}{2m} \frac{d^2\psi}{dx^2} = E\psi(x) \quad (\text{for } |x| > a). \quad (2.2)$$

For $E < 0$, we can find discrete solutions of the form

$$\psi(x) = c_{\pm} e^{\mp\kappa x}, \quad \text{where } c_{\pm} \in \mathbb{C}, \quad \kappa = \sqrt{-\frac{2mE}{\hbar^2}} \in \mathbb{R}^+. \quad (2.3)$$

By choosing $e^{-\kappa x}$ for $x > a$, and $e^{+\kappa x}$ for $x < -a$, the wavefunction vanishes exponentially away from the potential well, so it is normalizable to unity. These solutions are called bound states. There is also a lower energy bound, $E \geq -U$, stemming from the variational principle. Hence, the bound states form a discrete set of eigenenergies within the range

$$-U \leq E < 0. \quad (2.4)$$

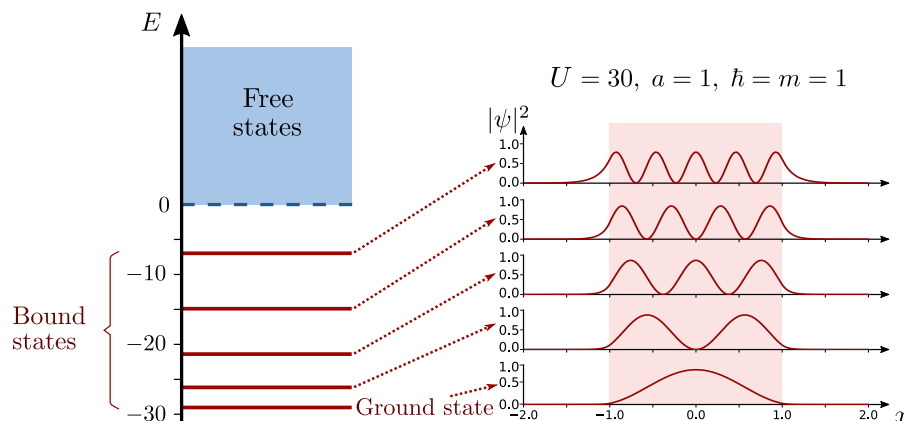
For $E > 0$, we cannot construct exponentially localized solutions. We instead consider

$$\psi(x) = \begin{cases} \alpha_- e^{ikx} + \beta_- e^{-ikx}, & x < -a \\ \text{(something)}, & -a < x < a \\ \alpha_+ e^{ikx} + \beta_+ e^{-ikx}, & x > a, \end{cases} \quad \text{where } k = \sqrt{\frac{2mE}{\hbar^2}} \in \mathbb{R}^+. \quad (2.5)$$

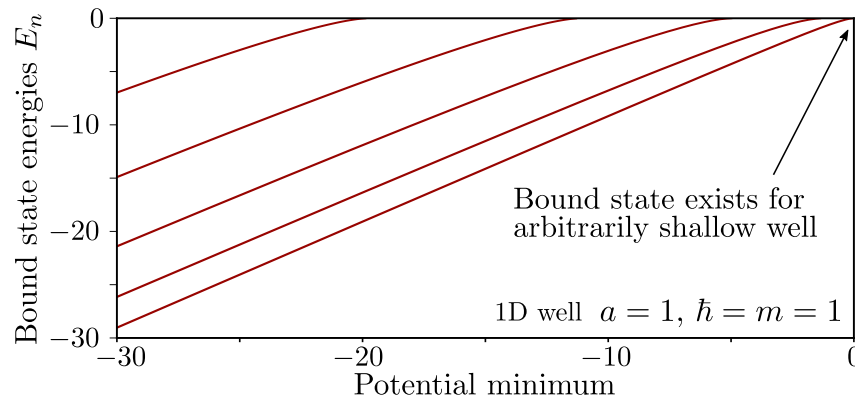
Such a solution is called a free state. It cannot be normalized to unity since $\int_{-\infty}^{\infty} |\psi(x)|^2 dx$ diverges. However, it is “almost normalizable” in the sense that $|\psi|^2$ does not blow up as $|x| \rightarrow \pm\infty$. We can thus treat it as a valid quantum wavefunction, on the same footing as plane waves (the wavefunctions for momentum eigenstates).

For each E , we can find coefficients α_{\pm} and β_{\pm} for Eq. (2.5) so as to satisfy the Schrödinger wave equation. It turns out that these four coefficients are not independent; for example, if we fix α_{\pm} , that uniquely determines β_{\pm} (see Appendix B). As this can be done for all $E \geq 0$, Eq. (2.5) represents a continuous family of free state solutions.

The following figure shows numerically obtained results for a square well with $U = 30$ and $a = 1$ (in units where $\hbar = m = 1$). The energy spectrum is shown on the left side. There are five discrete bound states; their plots of $|\psi|^2$ versus x are shown on the right side. These results were computed using the transfer matrix method described in Appendix B.

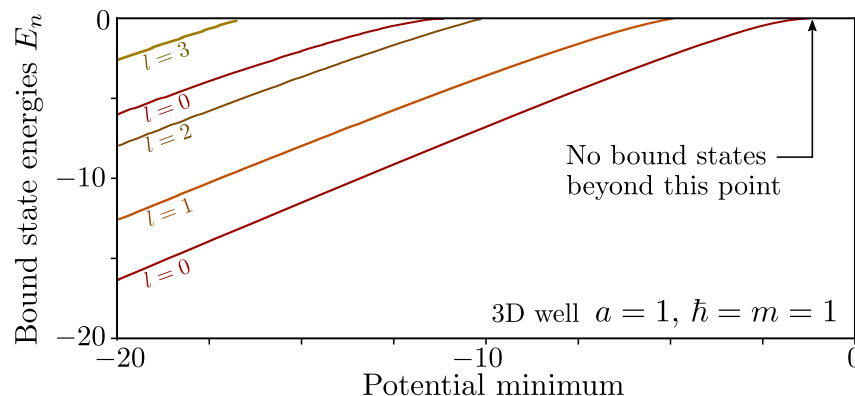


The number of bound states is not fixed. In the figure below, we vary the potential minimum $-U$ (with fixed $a = 1$), and plot the bound state energies:



For $U = 30$, there are five bound states. As the well gets shallower, these disappear one by one, with only one surviving as $U \rightarrow 0$. (There is a theorem stating that any 1D attractive potential, no matter how weak, supports at least one bound state; see [Exercise 1](#).)

Many features of this simple model are generalizable to more complicated cases, including higher spatial dimensions. One notable difference is that in 3D, it is possible for an attractive potential to be too weak to support a bound state (i.e., its binding energy cannot overcome the zero-point energy of a prospective ground state). The figure below shows an example based on a uniform 3D spherically symmetric well (the l labels are angular momentum quantum numbers). To learn more about this phenomenon, refer to [Exercise 2](#).

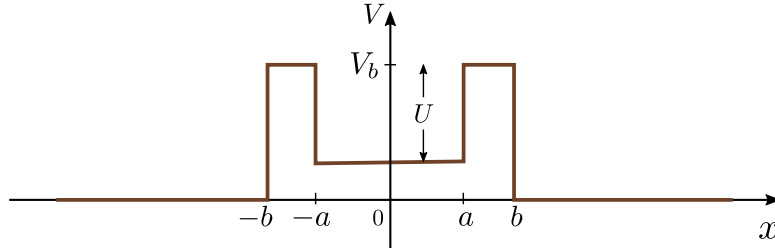


2.2. QUASI-BOUND STATES AND RESONANCES

For the 1D finite square well, there is a clear distinction between bound and free states. However, certain states, called “**quasi-bound states**”, can straddle the two cases. As we shall see, they play a particularly important role in scattering experiments.

The figure below shows an example of a potential function that hosts quasi-bound states. In the exterior region $|x| > b$, the potential vanishes. Between $x = -b$ and $x = b$, there is a

barrier of height V_b , in the middle of which is a well of depth $U < V_b$ and width $2a$. Since $V \geq 0$ everywhere, there are no bound states: all eigenstates must be free states.



There is something intriguing about the central well. Consider an alternative potential

$$V_{\text{alt}}(x) = \begin{cases} V_b - U, & |x| < a, \\ V_b, & \text{otherwise,} \end{cases} \quad (2.6)$$

which is a finite square well. This should have at least one bound state, whose energy lies in the range $V_b - U < E < V_b$, and whose wavefunction $\psi(x)$ decays exponentially away from the well. Since V_{alt} differs from the original potential V only in the region $|x| > b$, where $\psi(x)$ is small, this should also serve as an *approximate* solution for V !

In the context of the original scattering potential V , such a solution is called a **quasi-bound state**. It acts like a bound state, but is not actually a bound state for V (since it is not an exact eigenstate). In fact, as noted above, V lacks true bound states.

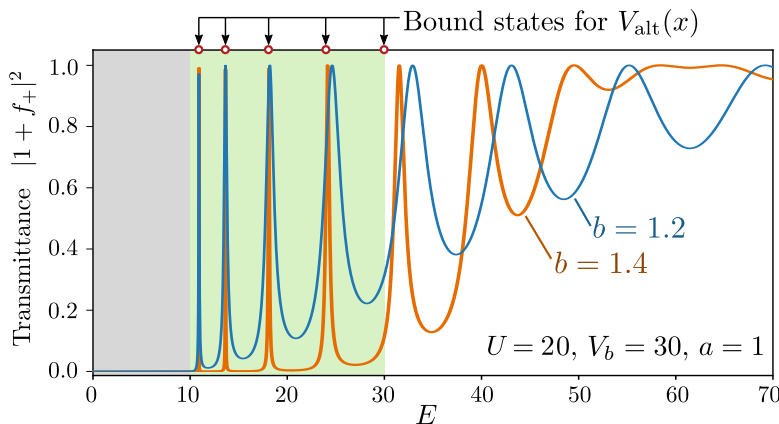
We can also analyze the situation using the scattering framework from Chapter 1. Consider an incident particle of energy $E > 0$ whose wavefunction is

$$\psi_i(x) = \Psi_i e^{ik_i x}. \quad (2.7)$$

This produces a scattered wavefunction, which takes the following form in the exterior region:

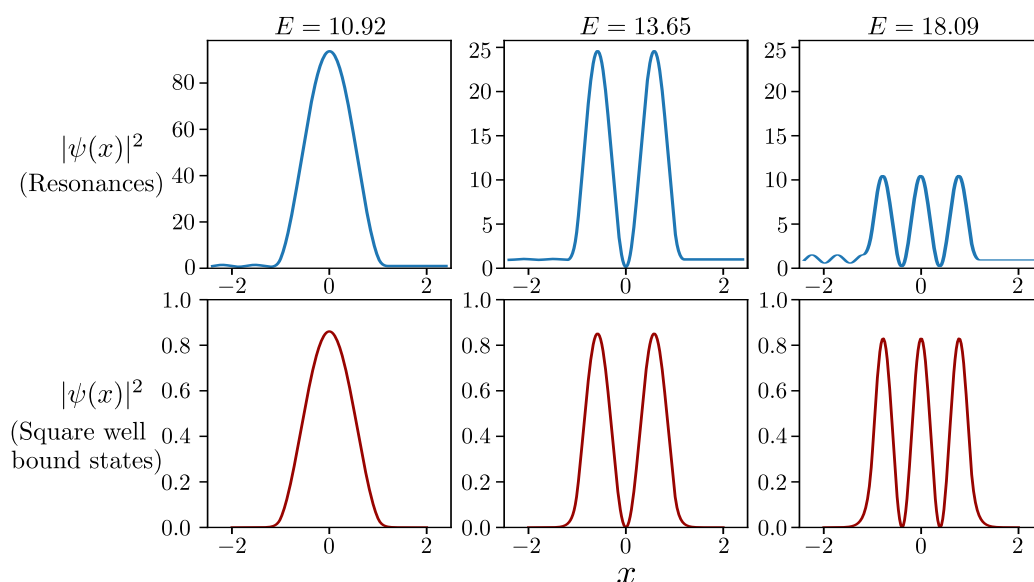
$$\psi_s(x) = \Psi_i \times \begin{cases} f_- e^{-ik_i x}, & x \leq -b \\ f_+ e^{ik_i x}, & x \geq b. \end{cases} \quad (2.8)$$

We can obtain f_{\pm} via the transfer matrix method (see Appendix B). The figure below shows numerical results obtained for $U = 20$, $V_b = 30$, $a = 1$, and $b \in \{1.2, 1.4\}$, with $\hbar = m = 1$.



The vertical axis shows the **transmittance** $|1 + f_+|^2$, which is the probability for the particle to pass through the scatterer. The horizontal axis is the particle energy E . Unsurprisingly, for $E < V_b - U$ the transmittance approaches zero, and for $E \gtrsim V_b$ it approaches unity. For $V_b - U < E \lesssim V_b$, the transmittance forms a series of narrow peaks; for larger b (i.e., when the central well is more isolated from the exterior space), the peaks are narrower. At the top of the figure, we have also plotted the bound state energies for the square well potential $V_{\text{alt}}(x)$. These energies closely match the locations of the transmittance peaks!

Looking at the wavefunction reveals other interesting features. Below, we plot $|\psi(x)|^2$ versus x at the energies of the first three transmittance peaks, along with the corresponding quasi-bound state wavefunctions. At each peak, observe that: (i) $|\psi(x)|^2$ is very large in the potential region, and (ii) its shape is very similar to the corresponding quasi-bound state.



We interpret the situation as follows: at certain energies, an incident particle ends up spending a long time trapped inside the scatterer, taking on many of the characteristics of a bound state. But unlike a true bound state, it is not trapped forever. Eventually, it leaks out of the scatterer and escapes to infinity.

The enhancement of $|\psi|^2$ by the presence of a quasi-bound state is called **resonance**, and it is closely analogous to the phenomenon of the same name in classical mechanics. When a damped harmonic oscillator is subjected to a periodic driving force, it undergoes steady-state oscillation at the driving frequency. If this matches the frequency of one of the oscillator’s “normal modes”, the oscillation amplitude grows large, as Galileo noted in the epigraph of this chapter.

In the quantum scattering experiment, the incident wavefunction plays the role of the driving force, E acts as the driving frequency, and quasi-bound states act like the normal modes. Oftentimes, scattering experiments are conducted for the express purpose of locating and studying resonances. When a resonance is found, it can be used to deduce various important information about the scatterer, as we shall see in the next few sections.

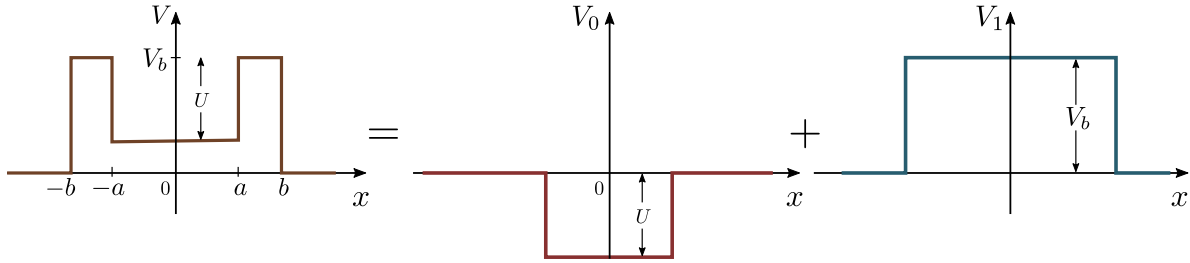
2.3. GREEN'S FUNCTION ANALYSIS OF SCATTERING RESONANCES

The Green's function formalism from Chapter 1, Sec. 1.5, provides a powerful and general way to understand quasi-bound states and resonances. Notably, this framework applies not only to 1D models, but works for higher dimensions as well.

Let $\hat{H} = \hat{T} + \hat{V}$ be the Hamiltonian of a system supporting resonances, where \hat{T} is the kinetic energy operator and \hat{V} is the potential operator. We decompose the potential into

$$\hat{V} = \hat{V}_0 + \hat{V}_1, \quad (2.9)$$

where \hat{V}_0 is a “confining potential” that supports a bound state, and \hat{V}_1 is a “deconfining potential” that turns the bound state into a quasi-bound state. For example, the potential functions for the 1D model of the previous section are shown below:



(Note that this 1D case is just an illustration; Eq. (2.9) applies to higher dimensions too.)

When the potential is just \hat{V}_0 , let there be a bound state $|\varphi\rangle$ with energy E_0 . Furthermore, let us assume that the potential supports a continuum of free states $\{|\psi_k\rangle\}$ with energies $\{E_k\}$, where k is some continuous index for labeling the free states (we will discuss what this index might represent later). The states satisfy the Schrödinger equation

$$(\hat{T} + \hat{V}_0)|\varphi\rangle = E_0|\varphi\rangle \quad (2.10)$$

$$(\hat{T} + \hat{V}_0)|\psi_k\rangle = E_k|\psi_k\rangle, \quad (2.11)$$

along with the orthogonality and completeness relations

$$\langle\varphi|\psi_k\rangle = 0, \quad |\varphi\rangle\langle\varphi| + \sum_k |\psi_k\rangle\langle\psi_k| = \hat{I}. \quad (2.12)$$

Here, \sum_k represents a sum over all free states. Since the free states form a continuum, this ought to be expressed as an integral, similar to how we treat momentum eigenstates (see Chapter 1). But, for the moment, we write it as a sum for ease of presentation.

Let us treat \hat{V} as a scattering potential, and compute the Green's function. According to Dyson's equations, the Green's function for the full system is

$$\hat{G} = \hat{G}_0 + \hat{G}\hat{V}_1\hat{G}_0, \quad (2.13)$$

where

$$\hat{G}_0(E) = \lim_{\varepsilon \rightarrow 0^+} \left(E - \hat{T} - \hat{V}_0 + i\varepsilon \right)^{-1} \quad (2.14)$$

is the causal Green's function. Note that Eq. (2.13) is exact, not an approximation. If we can obtain $\hat{G}(E)$, we can determine the scattering amplitudes.

Let us find the matrix elements of $\hat{G}(E)$ by using $|\varphi\rangle$ and $\{|\psi_k\rangle\}$ as a convenient basis. Note, however, that this is *not* the energy eigenbasis of \hat{H} .

As usual when dealing with Dyson's equations, we must beware of the fact that \hat{G} appears on both the left- and right-hand sides. We judiciously insert a resolution of the identity as follows:

$$\hat{G} = \hat{G}_0 + \hat{G}\hat{I}\hat{V}_1\hat{G}_0 = \hat{G}_0 + \hat{G}\left(|\varphi\rangle\langle\varphi| + \sum_k |\psi_k\rangle\langle\psi_k|\right)\hat{V}_1\hat{G}_0. \quad (2.15)$$

We then compute the matrix element $\langle\varphi|\cdots|\varphi\rangle$ for both sides:

$$\begin{aligned} \langle\varphi|\hat{G}|\varphi\rangle &= \langle\varphi|\hat{G}_0|\varphi\rangle + \langle\varphi|\hat{G}|\varphi\rangle\langle\varphi|\hat{V}_1\hat{G}_0|\varphi\rangle + \sum_k \langle\varphi|\hat{G}|\psi_k\rangle\langle\psi_k|\hat{V}_1\hat{G}_0|\varphi\rangle \\ \langle\varphi|\hat{G}|\varphi\rangle\left(1 - \langle\varphi|\hat{V}_1\hat{G}_0|\varphi\rangle\right) &= \langle\varphi|\hat{G}_0|\varphi\rangle + \sum_k \langle\varphi|\hat{G}|\psi_k\rangle\langle\psi_k|\hat{V}_1\hat{G}_0|\varphi\rangle \\ \lim_{\varepsilon\rightarrow 0^+} \langle\varphi|\hat{G}|\varphi\rangle\left(1 - \frac{\langle\varphi|\hat{V}_1|\varphi\rangle}{E - E_0 + i\varepsilon}\right) &= \lim_{\varepsilon\rightarrow 0^+} \frac{1}{E - E_0 + i\varepsilon}\left(1 + \sum_k \langle\varphi|\hat{G}|\psi_k\rangle\langle\psi_k|\hat{V}_1|\varphi\rangle\right) \\ \lim_{\varepsilon\rightarrow 0^+} \langle\varphi|\hat{G}|\varphi\rangle\left(E - E_0 - \langle\varphi|\hat{V}_1|\varphi\rangle + i\varepsilon\right) - \sum_k \langle\varphi|\hat{G}|\psi_k\rangle\langle\psi_k|\hat{V}_1|\varphi\rangle &= 1. \end{aligned} \quad (2.16)$$

Similarly, computing the matrix element $\langle\varphi|\cdots|\psi_k\rangle$ gives

$$\begin{aligned} \langle\varphi|\hat{G}|\psi_k\rangle &= \langle\varphi|\hat{G}_0|\psi_k\rangle + \langle\varphi|\hat{G}|\varphi\rangle\langle\varphi|\hat{V}_1\hat{G}_0|\psi_k\rangle + \sum_{k'} \langle\varphi|\hat{G}|\psi_{k'}\rangle\langle\psi_{k'}|\hat{V}_1\hat{G}_0|\psi_k\rangle \\ &= \lim_{\varepsilon\rightarrow 0^+} (E - E_k + i\varepsilon)^{-1} \left(\langle\varphi|\hat{G}|\varphi\rangle\langle\varphi|\hat{V}_1|\psi_k\rangle + \sum_{k'} \langle\varphi|\hat{G}|\psi_{k'}\rangle\langle\psi_{k'}|\hat{V}_1|\psi_k\rangle \right). \end{aligned}$$

So far, the equations have been exact, but now we apply an approximation: in the last line of the above equation, let the factor of $\langle\varphi|\hat{G}|\varphi\rangle$ be large, so that the first term in the sum is dominant. It will be shown below that $\langle\varphi|\hat{G}|\varphi\rangle$ being large is precisely the resonance condition, so this approximation will be self-consistent. Thus, we obtain

$$\langle\varphi|\hat{G}|\psi_k\rangle \approx \lim_{\varepsilon\rightarrow 0^+} \frac{\langle\varphi|\hat{G}|\varphi\rangle\langle\varphi|\hat{V}_1|\psi_k\rangle}{E - E_k + i\varepsilon}. \quad (2.17)$$

Combining this with Eq. (2.16) gives

$$\lim_{\varepsilon\rightarrow 0^+} \left[\langle\varphi|\hat{G}|\varphi\rangle\left(E - E_0 - \langle\varphi|\hat{V}_1|\varphi\rangle + i\varepsilon\right) - \sum_k \frac{\langle\varphi|\hat{G}|\varphi\rangle\langle\varphi|\hat{V}_1|\psi_k\rangle}{E - E_k + i\varepsilon} \langle\psi_k|\hat{V}_1|\varphi\rangle \right] \approx 1.$$

We finally arrive at the result

$$\langle\varphi|\hat{G}(E)|\varphi\rangle \approx \frac{1}{E - E_0 - \langle\varphi|\hat{V}_1|\varphi\rangle - \Sigma(E)} \quad (2.18)$$

$$\text{where } \Sigma(E) \equiv \lim_{\varepsilon\rightarrow 0^+} \sum_k \frac{|\langle\psi_k|\hat{V}_1|\varphi\rangle|^2}{E - E_k + i\varepsilon}. \quad (2.19)$$

2.4. THE SELF ENERGY

The enigmatic $\Sigma(E)$ appearing in the denominator in Eq. (2.18) is called the **self energy**. If we put aside its dependence on E and treat it as a constant, Eq. (2.18) looks like the Green's function of a system with an energy eigenstate $|\varphi\rangle$ of energy

$$E_0 + \langle\varphi|\hat{V}_1|\varphi\rangle + \Sigma.$$

We can interpret this as the energy of the quasi-bound state. The first term is the energy of the original bound state, the second term is a straightforward energy shift coming from the deconfining potential \hat{V}_1 , and the third term is the self energy. According to Eq. (2.19), Σ arises from the interplay between $|\varphi\rangle$ and the free states $\{|\psi_k\rangle\}$. The quasi-bound state disturbs the free states, which collectively exert a back-action that shifts its energy.

There is an important complication: Σ turns out to be complex, not real! From Eq. (2.19),

$$\begin{aligned} \text{Im}[\Sigma(E)] &= \lim_{\varepsilon \rightarrow 0^+} \sum_k \left| \langle\psi_k|\hat{V}_1|\varphi\rangle \right|^2 \text{Im} \left(\frac{1}{E - E_k + i\varepsilon} \right) \\ &= - \sum_k \left| \langle\psi_k|\hat{V}_1|\varphi\rangle \right|^2 \left[\lim_{\varepsilon \rightarrow 0^+} \frac{\varepsilon}{(E - E_k)^2 + \varepsilon^2} \right]. \end{aligned} \quad (2.20)$$

The quantity in the square brackets is a Lorentzian function of width ε . The area under the curve is π , independent of ε , so we can use the limiting expression

$$\lim_{\varepsilon \rightarrow 0^+} \frac{\varepsilon}{x^2 + \varepsilon^2} = \pi\delta(x). \quad (2.21)$$

Therefore,

$$\text{Im}[\Sigma(E)] = -\pi \sum_k \left| \langle\psi_k|\hat{V}_1|\varphi\rangle \right|^2 \delta(E - E_k) < 0. \quad (2.22)$$

What does it mean for an energy to be complex? If a quantum state has energy E , its time dependence goes as $\exp(-iEt/\hbar)$. For $E = \mathcal{E} + i\Gamma$, the time evolution factor is

$$e^{-i\mathcal{E}t/\hbar} e^{\Gamma t/\hbar}.$$

Since $\text{Im}[\Sigma] < 0$, the quasi-bound state is decaying exponentially with time. This matches our description of it as a localized state that is *almost* an energy eigenstate, but not exactly one—so, after some time, it escapes the scatterer and disappears to infinity.

2.5. SCATTERING RESONANCES

In Chapter 1, Sec. 1.7, we derived the following relationship between the Green's function and the scattering amplitude f :

$$f(\mathbf{k} \rightarrow \mathbf{k}') \propto \langle\mathbf{k}'|\hat{V}|\mathbf{k}\rangle + \langle\mathbf{k}'|\hat{V}\hat{G}\hat{V}|\mathbf{k}\rangle. \quad (2.23)$$

Here, $|\mathbf{k}\rangle$ and $|\mathbf{k}'\rangle$ are incident and scattered plane wave states satisfying $|\mathbf{k}| = |\mathbf{k}'|$. The first term describes the lowest-order scattering process (the first Born approximation). The second term contains second- and higher-order scattering processes.

By inserting resolutions of the identity between each \hat{V} and \hat{G} operator in the second term, we find that f contains a contribution of the form

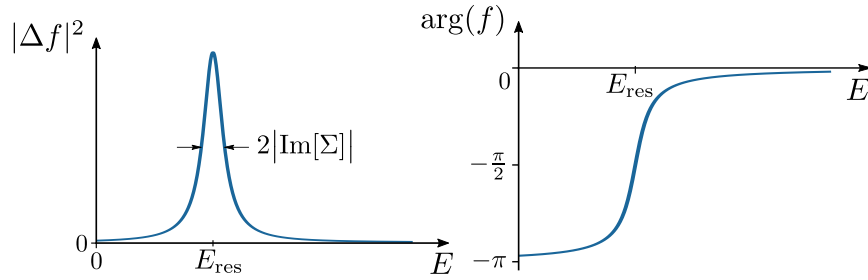
$$\Delta f(\mathbf{k} \rightarrow \mathbf{k}') \propto \langle \mathbf{k}' | \hat{V} | \varphi \rangle \langle \varphi | \hat{G} | \varphi \rangle \langle \varphi | \hat{V} | \mathbf{k} \rangle = \frac{\langle \mathbf{k}' | \hat{V} | \varphi \rangle \langle \varphi | \hat{V} | \mathbf{k} \rangle}{E - E_{\text{res}} - i \text{Im}[\Sigma]}, \quad (2.24)$$

where

$$E_{\text{res}} \equiv E_0 + \langle \varphi | \hat{V}_1 | \varphi \rangle + \text{Re}[\Sigma] \in \mathbb{R}. \quad (2.25)$$

At resonance, the denominator is small so Δf is the dominant part of f . It is worth noting that Δf contains contributions from all terms in the Born series, not just low-order terms.

The figure below shows the energy dependence of Δf , according to Eq. (2.24):



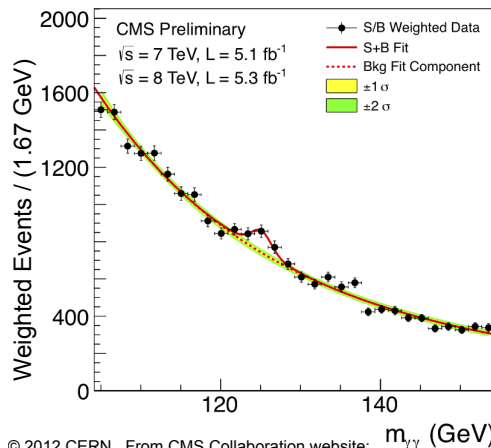
The graph of $|\Delta f|^2$ versus E forms a Lorentzian curve centered at E_{res} . The width of the peak can be characterized by the full-width at half-maximum (FWHM), the spacing between the two energies where $|\Delta f|^2$ has half its maximum value, which can be calculated to be

$$\delta E^{(\text{FWHM})} = 2 |\text{Im}[\Sigma]|. \quad (2.26)$$

(Note: we showed earlier that $\text{Im}[\Sigma] < 0$.) The smaller the decay rate, the sharper the peak.

The phase $\arg[\Delta f]$ also contains useful information. As E crosses E_{res} from below, the phase increases by π . The shift also occurs over an energy width of $\sim |\text{Im}[\Sigma]|$.

These resonant features—peaks and/or phase shifts—are sought after in many kinds of real-world scattering experiments. Often, they are overlaid on a “background” caused by non-resonant processes. This can be seen, for example, in the plot below from the CMS experiment at the Large Hadron Collider (LHC), declaring the experimental observation of the Higgs boson in 2012.



© 2012 CERN. From CMS Collaboration website:
<http://cms.web.cern.ch/news/observation-new-particle-mass-125-gev>

2.6. FERMI'S GOLDEN RULE

In the previous sections, we have seen that the width of a resonance is determined by the decay rate of a quasi-bound state, which is given by the imaginary part of its self energy. Now, we will derive a simple and powerful formula for approximating it in many circumstances, called **Fermi's Golden Rule**.

Suppose we initialize the particle, at time $t = 0$, to a quasi-bound state $|\varphi\rangle$. As $|\varphi\rangle$ is not an eigenstate of the Hamiltonian, the particle does not remain in that state forever. To quantify the “decay” of the quasi-bound state, we imagine performing a measurement that has $|\varphi\rangle$ as one of its eigenstates, at time $t > 0$. The probability that the particle is observed to still be in state $|\varphi\rangle$ is

$$P(t) = \left| \langle \varphi | \exp\left(-i\hat{H}t/\hbar\right) |\varphi\rangle \right|^2. \quad (2.27)$$

To help us calculate $P(t)$, let us define

$$f(t) = \begin{cases} \langle \varphi | \exp\left(-i\hat{H}t/\hbar\right) |\varphi\rangle e^{-\varepsilon t}, & t \geq 0 \\ 0, & t < 0, \end{cases} \quad (2.28)$$

where $\varepsilon \in \mathbb{R}^+$. For $t \geq 0$ and $\varepsilon \rightarrow 0^+$, we see that $|f(t)|^2 \rightarrow P(t)$. The reason we deal with $f(t)$ is that it is more well-behaved than the actual amplitude $\langle \varphi | \exp(-i\hat{H}t/\hbar) |\varphi\rangle$. The function is designed so that (i) it vanishes at times prior to start of the experiment, and (ii) it vanishes as $t \rightarrow \infty$ due to the regulator ε . The latter condition is based on our expectation that the bound state should decay permanently into the continuum of free states, and should never be repopulated by waves “bouncing back” from infinity.

To find $f(t)$, we first take its Fourier transform,

$$F(\omega) = \int_{-\infty}^{\infty} dt e^{i\omega t} f(t) = \int_0^{\infty} dt e^{i(\omega+i\varepsilon)t} \langle \varphi | e^{-i\hat{H}t/\hbar} |\varphi\rangle. \quad (2.29)$$

Now insert a resolution of the identity, $\hat{I} = \sum_n |n\rangle\langle n|$, where $\{|n\rangle\}$ denotes the exact eigenstates of \hat{H} (for free states, the sum goes to an integral in the usual way):

$$\begin{aligned} F(\omega) &= \int_0^{\infty} dt e^{i(\omega+i\varepsilon)t} \sum_n \langle \varphi | e^{-i\hat{H}t/\hbar} |n\rangle \langle n | \varphi \rangle \\ &= \sum_n \langle \varphi | n \rangle \left(\int_0^{\infty} dt \exp\left[i \left(\omega - \frac{E_n}{\hbar} + i\varepsilon \right) t \right] \right) \langle n | \varphi \rangle \\ &= \sum_n \langle \varphi | n \rangle \frac{i}{\omega - \frac{E_n}{\hbar} + i\varepsilon} \langle n | \varphi \rangle \\ &= i\hbar \langle \varphi | \left(\hbar\omega - \hat{H} + i\hbar\varepsilon \right)^{-1} | \varphi \rangle. \end{aligned} \quad (2.30)$$

In the third line, the regulator ε removes the contribution from the $t \rightarrow \infty$ limit. Hence,

$$\lim_{\varepsilon \rightarrow 0^+} F(\omega) = i\hbar \langle \varphi | \hat{G}(\hbar\omega) | \varphi \rangle, \quad (2.31)$$

where \hat{G} is our old friend the causal Green's function (see Chapter 1, Sec. 1.6). Its appearance can be traced to Eq. (2.28), which defines $f(t)$ to be nonzero only for $t \geq 0$.

In Section 2.5, we saw that when the system is at or close to resonance,

$$\langle \varphi | \hat{G}(E) | \varphi \rangle \approx \frac{1}{E - E_{\text{res}} - i\text{Im}[\Sigma]}, \quad (2.32)$$

where E_{res} is the resonance energy, and Σ is the self energy of the quasi-bound state. Using this, we can perform an inverse Fourier transform to retrieve $f(t)$:

$$\begin{aligned} \lim_{\epsilon \rightarrow 0^+} f(t) &= \lim_{\epsilon \rightarrow 0^+} \int_{-\infty}^{\infty} \frac{d\omega}{2\pi} e^{-i\omega t} F(\omega) \\ &\approx \frac{i}{2\pi} \int_{-\infty}^{\infty} d\omega \frac{e^{-i\omega t}}{\omega - (E_{\text{res}} + i\text{Im}[\Sigma])/\hbar} \\ &\approx \exp\left(-\frac{iE_{\text{res}}t}{\hbar}\right) \exp\left(-\frac{|\text{Im}[\Sigma]|}{\hbar} t\right), \end{aligned} \quad (2.33)$$

where $\text{Im}[\Sigma]$ is to be evaluated at $E = E_{\text{res}}$. Thus,

$$P(t) = e^{-\kappa t}, \quad \text{where } \kappa = \frac{2|\text{Im}[\Sigma(E_{\text{res}})]|}{\hbar}. \quad (2.34)$$

The quasi-bound state decays exponentially, with a decay rate proportional to $|\text{Im}[\Sigma]|$.

We previously derived a formula for $\text{Im}[\Sigma]$, Eq. (2.22), reproduced here for convenience:

$$\text{Im}[\Sigma(E)] = -\pi \sum_k |\langle \psi_k | \hat{V}_1 | \varphi \rangle|^2 \delta(E - E_k). \quad (2.35)$$

In the sum over k , each term is a non-negative real number consisting of two factors: (i) a k -dependent “weight” $|\langle \psi_k | \hat{V}_1 | \varphi \rangle|^2$, and (ii) a delta function, which vanishes unless $E_k = E$. Because only a subset of the free states are relevant to the sum, it is convenient to define

$$\overline{|\langle \psi_{k(E)} | \hat{V}_1 | \varphi \rangle|^2},$$

which is the average weight over the participating free states (i.e., those with $E = E_k$). Then we can approximate Eq. (2.35) by pulling the weights out of the sum:

$$\text{Im}[\Sigma(E)] \approx -\pi \overline{|\langle \psi_{k(E)} | \hat{V}_1 | \varphi \rangle|^2} \sum_k \delta(E - E_k). \quad (2.36)$$

This allows us to write the decay rate in Eq. (2.34) as

$$\kappa \approx \frac{2\pi}{\hbar} \overline{|W|^2} \rho(E_{\text{res}}), \quad \text{where } \begin{cases} W = \langle \psi_k | \hat{V}_1 | \varphi \rangle \\ \rho(E) = \sum_k \delta(E - E_k). \end{cases} \quad (2.37)$$

This result is called **Fermi’s golden rule**. It states that the decay rate of a quasi-bound state is determined by the product of two real factors:

- $\overline{|\mathcal{W}|^2}$, which is obtained by taking the absolute square of the **transition amplitude** $\langle \psi_k | \hat{V}_1 | \varphi \rangle$, and averaging over available free states (i.e., the free states meeting the resonance condition $E_k = E_{\text{res}}$). This characterizes how strongly the quasi-bound state couples, on average, to the available free states.
- $\rho(E_{\text{res}})$, which is the number of free states per unit energy at energy E_{res} . This says that the decay rate is proportional to the number of available free states.

Typically, these two factors are estimated by making further approximations.

One very common approximation is to treat the free states as plane waves. In this case, we take the k labels to be d -dimensional wave-vectors. As the wave-vectors are continuous, we convert the sum over k into an integral in the usual way, by defining the discretization step $dk = 2\pi/L$ where $L \rightarrow \infty$ (see Chapter 1, Sec. 1.2):

$$\begin{aligned} \rho(E) &= \sum_k \delta(E - E_k) \\ &= L^d \underbrace{\int \frac{d^d k}{(2\pi)^d} \delta(E - E_k)}_{\equiv \mathcal{D}(E)}. \end{aligned} \quad (2.38)$$

The **density of states** $\mathcal{D}(E)$ counts the number of free states of energy E , per unit energy and per unit volume. Note that it has different dimensions from $\rho(E)$. We also need to re-normalize the transition amplitude, via the usual delta-normalization convention:

$$|\psi_k\rangle^{(\text{new})} = \left(\frac{L}{2\pi}\right)^{d/2} |\psi_k\rangle^{(\text{old})} \quad (2.39)$$

$$\Rightarrow \langle \psi_k | \hat{V}_1 | \varphi \rangle^{(\text{old})} = \left(\frac{2\pi}{L}\right)^{d/2} \langle \psi_k | \hat{V}_1 | \varphi \rangle^{(\text{new})}. \quad (2.40)$$

Plugging Eq. (2.38) and (2.40) into (2.37), we can re-state Fermi's golden rule as

$$\kappa \approx \frac{2\pi}{\hbar} \overline{|\mathcal{W}|^2} \mathcal{D}(E_{\text{res}}), \quad \text{where} \quad \begin{cases} \mathcal{W} = (2\pi)^{d/2} \langle \psi_k | \hat{V}_1 | \varphi \rangle \\ \mathcal{D}(E) = \int \frac{d^d k}{(2\pi)^d} \delta(E - E_k). \end{cases} \quad (2.41)$$

Here, $\overline{|\mathcal{W}|^2}$ is averaged over all plane waves satisfying the resonance condition $E_k = E$. Note that the L factors in Eq. (2.38) and (2.40) do not appear in the result (2.41), as they have cancelled each other out.

2.7. FERMI'S GOLDEN RULE IN A 1D MODEL

Let us apply Fermi's golden rule to the simple 1D model of Section 2.2. The potential is

$$V(x) = V_0(x) + V_1(x), \quad \text{where} \quad \begin{cases} V_0(x) = -U \Theta(a - |x|) \\ V_1(x) = V_b \Theta(b - |x|) \\ 0 < U < V_b. \end{cases} \quad (2.42)$$

The finite square well $V_0(x)$ supports one or more bound states; for simplicity, we focus on the ground state, whose energy is denoted by E_0 (where $-U < E_0 < 0$). Its wavefunction is

$$\varphi(x) = \begin{cases} \mathcal{A} \cos(qx), & |x| < a \\ \mathcal{B} \exp(-\eta|x|), & |x| \geq a, \end{cases} \quad (2.43)$$

where \mathcal{A} and \mathcal{B} are constants to be determined, and

$$q = \sqrt{\frac{2m}{\hbar^2}(E_0 + U)}, \quad \eta = \sqrt{\frac{2m}{\hbar^2}|E_0|}. \quad (2.44)$$

By matching $\varphi(x)$ and $d\varphi/dx$ across the $x = a$ interface, we can derive E_0 , \mathcal{A} , and \mathcal{B} . The details are left as an [exercise](#).

Having obtained $\varphi(x)$, we want the transition amplitude $\langle \psi_k | \hat{V}_1 | \varphi \rangle$, where $\psi_k(x)$ is a representative free eigenstate of $V_0(x)$ that the quasi-bound state decays to. We can estimate this with a series of tricks. First,

$$\langle \psi_k | \hat{V}_1 | \varphi \rangle = \int_{-\infty}^{\infty} dx \psi_k^*(x) V_1(x) \varphi(x) = V_b \int_{-b}^b dx \psi_k^*(x) \varphi(x). \quad (2.45)$$

Next, because $\psi_k(x)$ and $\varphi(x)$ are orthogonal,

$$\int_{-\infty}^{\infty} dx \psi_k^*(x) \varphi(x) = 0 \quad \Rightarrow \quad \int_{-b}^b dx \psi_k^*(x) \varphi(x) = - \int_{|x|>b} dx \psi_k^*(x) \varphi(x). \quad (2.46)$$

The integration range consists of two pieces, $x > b$ and $x < -b$, which can be interpreted as the decay of the quasi-bound state to the left or right. We assume these contribute equally to the escape probability, so

$$|\langle \psi_k | \hat{V}_1 | \varphi \rangle|^2 \approx 2V_b^2 \left| \int_b^{\infty} dx \psi_k^*(x) \varphi(x) \right|^2. \quad (2.47)$$

Outside the scatterer, the escaping free state is approximately an outgoing plane wave,

$$\psi_k(x) \approx \frac{e^{ikx}}{\sqrt{2\pi}}, \quad (2.48)$$

where

$$E_k = E_{\text{res}} \approx E_0 + V_b \quad \Rightarrow \quad k \approx \sqrt{\frac{2m}{\hbar^2}(E_0 + V_b)}. \quad (2.49)$$

Plugging Eqs. (2.43) and (2.48) into Eq. (2.47), and solving the integral, gives

$$|\langle \psi_k | \hat{V}_1 | \varphi \rangle|^2 \approx \frac{1}{\pi} V_b^2 \mathcal{B}^2 \frac{e^{-2\eta b}}{k^2 + \eta^2}. \quad (2.50)$$

The other quantity we need for Fermi's golden rule is the density of free states. This can be found by taking $E_k \approx \hbar^2 k^2 / 2m$, and performing a change of variables:

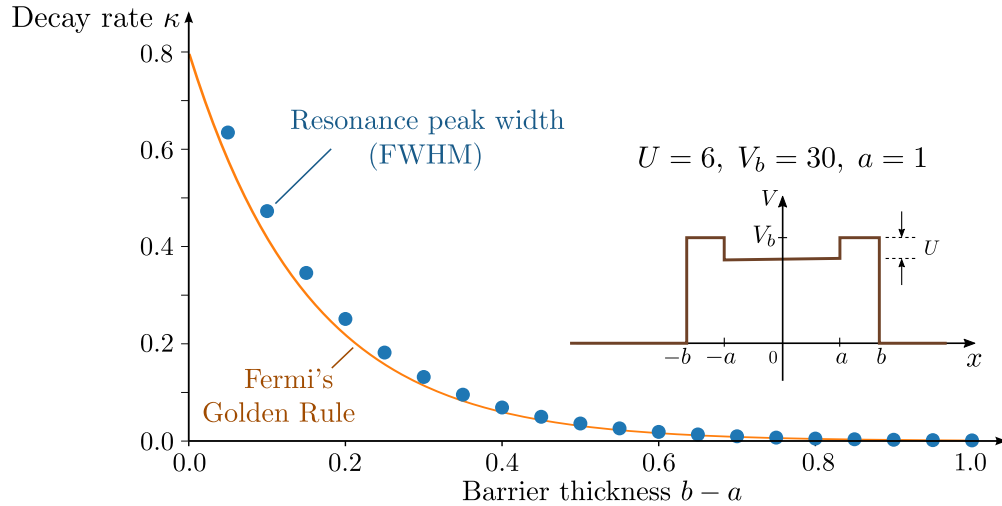
$$\mathcal{D}(E) = \int_{-\infty}^{\infty} \frac{dk}{2\pi} \delta\left(E - \frac{\hbar^2 k^2}{2m}\right) \quad (2.51)$$

$$= 2 \cdot \frac{1}{2\pi} \int_0^{\infty} dE' \frac{dk}{dE'} \delta(E - E') \quad (2.52)$$

$$= \sqrt{\frac{m}{2\pi^2 \hbar^2 E}}. \quad (2.53)$$

In Eq. (2.52), the factor of 2 accounts for the fact that for each E , both positive and negative k contribute to the density of states.

We can now plug Eqs. (2.50) and (2.53) into Fermi's golden rule, Eq. (2.41). The figure below shows results for $U = 6$, $V_b = 30$, and $a = 1$, with computational units $\hbar = m = 1$. The orange curve shows how κ , the decay rate from Fermi's golden rule, varies with the barrier thickness $b - a$. For comparison, the blue dots show the values of κ derived from the resonant scattering peak (see Section 2.5), by computing the transmittance using the transfer matrix method (see **Appendix B**) and numerically extracting the peak width.



The agreement is pretty good, especially considering the numerous approximations leading to the derivation of Fermi's golden rule! The behavior also matches our intuition: when the barrier thickness is large, the quasi-bound state should indeed decay more slowly.

In this simple 1D example, Fermi's golden rule is not especially useful since the scattering problem can be solved easily (see Appendix B). However, in higher dimensions, nonperturbative scattering problems are typically much less tractable. In such cases, Fermi's golden rule provides a very convenient way to estimate the widths of resonance peaks.

EXERCISES

1. Use the variational theorem to prove that a 1D potential well has at least one bound state. Assume that the potential $V(x)$ satisfies (i) $V(x) < 0$ for all x , and (ii) $V(x) \rightarrow 0$ for $x \rightarrow \pm\infty$. The Hamiltonian is

$$\hat{H} = -\frac{\hbar^2}{2m} \frac{d^2}{dx^2} + V(x). \quad (2.54)$$

Consider a (real) trial wavefunction

$$\psi(x; \gamma) = \left(\frac{2\gamma}{\pi}\right)^{1/4} e^{-\gamma x^2}. \quad (2.55)$$

Note that this can be shown to be normalized to unity, using Gauss' integral

$$\int_{-\infty}^{\infty} dx e^{-2\gamma x^2} = \sqrt{\frac{\pi}{2\gamma}}. \quad (2.56)$$

Now prove that

$$\begin{aligned}
 \langle E \rangle &= \int_{-\infty}^{\infty} dx \psi(x) \hat{H} \psi(x) \\
 &= \frac{\hbar^2}{2m} \int_{-\infty}^{\infty} dx \left(\frac{d\psi}{dx} \right)^2 + \int_{-\infty}^{\infty} dx V(x) \psi^2(x) \\
 &= A\sqrt{\gamma} \left[\sqrt{\gamma} + B \int_{-\infty}^{\infty} dx V(x) e^{-\gamma x^2} \right],
 \end{aligned} \tag{2.57}$$

where A and B are positive real constants to be determined. By looking at the quantity in square brackets in the limit $\gamma \rightarrow 0$, argue that $\langle E \rangle < 0$ in this limit. Hence, explain why this implies the existence of a bound state.

Finally, try generalizing this approach to the case of a 2D radially-symmetric potential well $V(x, y) = V(r)$, where $r = \sqrt{x^2 + y^2}$. Identify which part of the argument fails in 2D. [For a discussion of certain 2D potential wells that *do* always support bound states, similar to 1D potential wells, see Ref. [4].]

2. In this problem, you will investigate the existence of bound states in a 3D potential well that is finite, uniform, and spherically-symmetric. The potential function is

$$V(r, \theta, \phi) = -U\Theta(a - r), \tag{2.58}$$

where a is the radius of the spherical well, U is the depth, and (r, θ, ϕ) are spherical coordinates defined in the usual way.

The solution involves a variant of the partial wave analysis discussed in Appendix A. For $E < 0$, the Schrödinger equation reduces to

$$\begin{cases} (\nabla^2 + q^2)\psi(r, \theta, \phi) = 0 & \text{where } q = \sqrt{2m(E + U)/\hbar^2}, & \text{for } r \leq a \\ (\nabla^2 - \gamma^2)\psi(r, \theta, \phi) = 0 & \text{where } \gamma = \sqrt{-2mE/\hbar^2}, & \text{for } r \geq a. \end{cases} \tag{2.59}$$

For the first equation (called the Helmholtz equation), we seek solutions of the form

$$\psi(r, \theta, \phi) = f(r) Y_{\ell m}(\theta, \phi), \tag{2.60}$$

where $Y_{\ell m}(\theta, \phi)$ are [spherical harmonics](#), and the integers l and m are angular momentum quantum numbers satisfying $l \geq 0$ and $-l \leq m \leq l$. Substituting into the Helmholtz equation yields

$$r^2 \frac{d^2 f}{dr^2} + 2r \frac{df}{dr} + [q^2 r^2 - l(l + 1)] f(r) = 0, \tag{2.61}$$

which is the **spherical Bessel equation**. The solutions to this equation that are non-divergent at $r = 0$ are $f(r) = j_\ell(qr)$, where j_ℓ is called a **spherical Bessel function of the first kind**. Most numerical packages provide functions to calculate these (e.g., [scipy.special.spherical_jn](#) in [Scientific Python](#)).

Similarly, solutions for the second equation can be written as $\psi(r, \theta, \phi) = g(r) Y_{\ell m}(\theta, \phi)$, yielding an equation for $g(r)$ called the **modified spherical Bessel equation**. The

solutions which do not diverge as $r \rightarrow \infty$ are $g(r) = k_\ell(\gamma r)$, where k_ℓ is called a **modified spherical Bessel function of the second kind**. Again, this can be computed numerically (e.g., using `scipy.special.spherical_kn` in Scientific Python).

Using the above facts, show that the condition for a bound state to exist is

$$\frac{qj'_\ell(qa)}{j_\ell(qa)} = \frac{\gamma k'_\ell(\gamma a)}{k_\ell(\gamma a)}, \quad (2.62)$$

where j'_ℓ and k'_ℓ denote the derivatives of the relevant special functions, and q and γ depend on E and U as described above. Write a program to search for the bound state energies at any given a and U , and hence determine the conditions under which the potential does not support bound states.

3. In this problem, we will find the quasi-bound and free states for the model discussed in Section 2.7, and use it to calculate the decay rate according to Fermi's golden rule.

Let $\varphi(x)$ be the bound state of a square well of width $2a$ and depth U , and let E_0 be the energy. This state satisfies the 1D time-independent Schrödinger wave equation,

$$\left[-\frac{\hbar^2}{2m} \frac{d^2}{dx^2} + V(x) \right] \varphi(x) = E_0 \varphi(x), \quad (2.63)$$

where

$$V(x) = V_0(x) + V_1(x), \quad \text{where} \quad \begin{cases} V_0(x) = -U \Theta(a - |x|) \\ V_1(x) = V_b \Theta(b - |x|) \\ 0 < U < V_b. \end{cases} \quad (2.64)$$

Take the ansatz

$$\varphi(x) = \begin{cases} \mathcal{A} \cos(qx), & |x| < a \\ \mathcal{B} \exp(-\eta|x|), & |x| \geq a. \end{cases} \quad (2.65)$$

- (a) Using Eqs. (2.63)–(2.65), and the fact that both $\varphi(x)$ and $d\varphi/dx$ are continuous at $x = \pm a$, prove that E_0 can be obtained by solving the transcendental equation

$$q \tan(qa) = \eta, \quad \text{where} \quad \begin{cases} q = \sqrt{\frac{2m}{\hbar^2}(E_0 + U)} \\ \eta = \sqrt{\frac{2m}{\hbar^2}|E_0|}. \end{cases} \quad (2.66)$$

- (b) By using the fact that $\varphi(x)$ is normalized to unity, prove that

$$\mathcal{B}^2 = \frac{\exp(2\eta a)}{a} \left[\frac{1 + \sin(2qa)/2qa}{\cos^2(qa)} + \frac{1}{\eta a} \right]^{-1}. \quad (2.67)$$

- (c) Write a program to compute the decay rate based on Fermi's golden rule, by combining Eqs. (2.41), (2.50), (2.53), (2.66), and (2.67). Hence, reproduce the plot shown in Section 2.7.
- (d) Write a program to extract the decay rate from the width of the transmission peak, using the transfer matrix method (see Appendix B). Hence, investigate the accuracy of the Fermi's golden rule result for different values of U , V_b , and the other model parameters.

FURTHER READING

- [1] Bransden & Joachain, §4.4, 9.2–9.3, 13.4
- [2] Sakurai, §5.6, 7.7–7.8
- [3] R. Courant and D. Hilbert, *Methods of Mathematical Physics* vol. 1, Interscience (1953). [\[link\]](#)
- [4] B. Simon, *The bound state of weakly coupled Schrödinger operators in one and two dimensions*, *Annals of Physics* **97**, 279 (1976). [\[link\]](#)